# Stereochemistry and Stereodynamics of $\eta^6$-Hexaethylbenzene Transition Metal Complexes. Crystal and Molecular Structure of Dicarbonyl($\eta^6$-hexaethylbenzene)($\eta^2$-maleic anhydride)molybdenum(0) †

**Geoffrey Hunter * and Timothy J. R. Weakley**
*Department of Chemistry, The University, Dundee DD1 4HN*
**Kurt Mislow ***
*Department of Chemistry, Princeton University, Princeton, New Jersey 08544, U.S.A.*
**Margaret G. Wong**
*Department of Chemistry, Monash University, Clayton, Victoria 3168, Australia*

The variable-temperature 90.1-MHz $^{13}C$-{$^1H$} and/or 145.87-MHz $^{31}P$-{$^1H$} n.m.r. spectra of dicarbonyl($\eta^6$-hexaethylbenzene)(thiocarbonyl)chromium(0), (**4**), dicarbonyl($\eta^6$-hexaethylbenzene)(trimethylphosphine)chromium(0), (**5**), dicarbonyl($\eta^6$-hexaethylbenzene)(triethylphosphine)chromium(0), (**6**), dicarbonyl($\eta^6$-hexaethylbenzene)(triethylphosphine)molybdenum(0), (**7**), dicarbonyl($\eta^6$-hexaethylbenzene)(triphenyl phosphite)chromium(0), (**9**), dicarbonyl($\eta^6$-hexaethylbenzene)($\eta^2$-maleic anhydride)chromium(0), (**10**), dicarbonyl($\eta^6$-hexaethylbenzene)($\eta^2$-maleic anhydride)molybdenum(0), (**11**), and ($\eta^5$-cyclopentadienyl)($\eta^6$-hexaethylbenzene)iron(II) hexafluorophosphate, (**12**), have been observed and subjected to lineshape analysis. In a number of cases, multiple heb stereoisomers are found to coexist in equilibrium in solution at low temperatures. For all the hexaethylbenzene (heb) complexes examined, the n.m.r. spectra can be satisfactorily analysed without the need to invoke hindered rotation about the metal–arene bond and coalescence phenomena observed in the spectra are attributed to the onset of rapid rotation of the ethyl groups about the benzene ring and heb stereoisomerisation. Barriers to site exchange ($\Delta G^{\ddagger}$) of the ethyl groups are reported for a number of the heb complexes. The crystal and molecular structure for (**11**) has been determined and the co-ordinated heb has been found to adopt a 1,3,5-distal-2,4,6-proximal methyl conformation.

Hexaethylbenzene (heb) (**1**) is the smallest homosubstituted hexa-alkylbenzene, $C_6R_6$, in which are manifested the effects of steric overcrowding. Such a molecule can provide exceptional insights into the effect of intramolecular strain on ground-state structures and on internal mobility and there has therefore been interest in the static and dynamic stereochemistries both of this arene and of ($\eta^6$-heb)metal complexes.[1–3] Our own studies[1] have shown that: (*i*) the up–down alternation of ethyl groups actually observed in heb is only one of eight possible arrangements in which the methyl groups are located on one side or the other of the ring plane; (*ii*) of these arrangements only the four shown in Figure 1 are energetically favoured for tripodal [$ML_3$(heb)] complexes; (*iii*) increasing the size of the ligand L in complexes [$M(CO)_2L$(heb)] increases its non-bonding repulsive interactions with the heb moiety and decreases the number of proximal methyl groups; (*iv*) compensatory destabilisation tends to equalise the internal energies of the stereoisomeric heb complexes and thus leads to a situation where the favoured stereoisomers can coexist in equilibrium both in the crystal and in solution; (*v*) a single proximal methyl group is sufficient to ensure that the tripodal ligands eclipse the arene carbons; (*vi*) the stereoisomers interconvert by uncorrelated ethyl group rotation in both complexed and uncomplexed heb.

The remaining unquantified intramolecular exchange process in ($\eta^6$-heb)metal complexes involves rotation about the metal–arene bond. Although the magnitude of the barrier to such rotation in ($\eta^6$-arene)metal complexes has been a subject of general interest for some time, there are only two examples described in the literature where this process has been unequivocally shown to be slowed on the n.m.r. time-scale at accessible temperatures: [$Ru(CO)(C_6H_4Bu^t_2\text{-}p)(SiCl_3)_2$], where there are special steric factors,[4] and [$Cr(CO)_3(p\text{-}MeC_6H_4CHR)$]$^+$ (R = Me or $C_6H_4Me$-*p*), where there are special electronic factors.[5] It has recently been claimed[2a,c] that because of steric constraints, such rotation is slowed at accessible temperatures in [$Cr(CO)_2(CS)$(heb)] and, by implication, in [$M(CO)_3$(heb)]. However, we have adopted the more conservative position that the case for slowed rotation about the $\eta^6$-heb–metal bond remains not proven, and in a preliminary communication have advanced an alternative explanation of the low-temperature $^{13}C$ n.m.r. spectrum of [$Cr(CO)_2(CS)$(heb)].[1e]

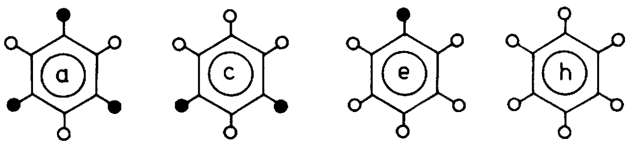

**Figure 1.** The four favoured heb stereoisomers for [$ML_3$(heb)] complexes. The metal atom is the point of reference and should be viewed as residing over the ring and above the plane of the paper. The filled (open) circles represent proximal (distal) methyl groups projecting towards (away from) the observer. We retain the previously introduced conformational descriptors (a)—(h) for the eight possible heb stereoisomers[1b]

The present paper reports a series of observations and interpretations on a broad range of problems relating to the stereochemistries of hexaethylbenzene complexes and presents our conclusions regarding the major intramolecular rotational processes of these compounds.

---

† *Supplementary data available* (No. SUP 56420, 3 pp.): thermal parameters. See Instructions for Authors, *J. Chem. Soc., Dalton Trans.*, 1986, Issue 1, pp. xvii—xx. Structure factors are available from the editorial office.

**Table 1.** Analytical figures for the previously unreported complexes

| Compound | | Found (%) C | Found (%) H | Formula | Required (%) C | Required (%) H |
|---|---|---|---|---|---|---|
| $[Cr(CO)_2(PMe_3)(heb)]$ | **(5)** | 64.5 | 8.6 | $C_{23}H_{39}CrO_2P$ | 64.2 | 9.1 |
| $[Mo(CO)_2(PEt_3)(heb)]$ | **(7)** | 60.9 | 8.5 | $C_{26}H_{45}MoO_2P$ | 60.5 | 8.7 |
| $[Cr(CO)_2(C_4H_2O_3)(heb)]$ | **(10)*** | 63.8 | 7.2 | $C_{24}H_{32}CrO_5$ | 63.7 | 7.1 |
| $[Mo(CO)_2(C_4H_2O_3)(heb)]$ | **(11)*** | 58.4 | 6.7 | $C_{24}H_{32}MoO_5$ | 58.1 | 6.5 |

* $C_4H_2O_3$ = maleic anhydride.

## Results and Discussion

*Static Stereochemistry of* ($\eta^6$-*Hexaethylbenzene*)*metal Complexes.*—Certain general trends are discernible from the crystal and molecular structures presently available for a number of complexes: $[Cr(CO)_3(heb)]$ **(2)**,[1a,b] $[Mo(CO)_3(heb)]$ **(3)**,[1a,b] $[Cr(CO)_2(CS)(heb)]$ **(4)**,[2a] $[Cr(CO)_2(PMe_3)(heb)]$ **(5)**,[1d] $[Cr(CO)_2(PEt_3)(heb)]$ **(6)**,[1a] $[Cr(CO)_2(PPh_3)(heb)]$ **(8)**,[1a,b] $[Mo(CO)_2(C_4H_2O_3)(heb)]$ **(11)**, and $[Fe(\eta^5\text{-}C_5H_5)(heb)]PF_6$ **(12)**.[2b] For the series of substituted phosphine ligands, in each case two heb stereoisomers are found in the crystal, either in exactly equal amounts with each stereoisomer occupying well defined positions in the unit cell as in **(6)**, or with the minor stereoisomer occurring as a random disorder in the cases of **(5)** and **(8)**. While crystal packing forces play an important role in determining which heb stereoisomers occur in the crystal, it is also apparent that increasing the effective size of the substituting ligand increases its non-bonding repulsive interactions with the ligand heb moiety and decreases the number of proximal methyl groups. Hence in the phosphine series there is good correlation between the cone angle[6] of the ligand and the stereochemistry adopted by the heb: $PMe_3$, cone angle 118°, major stereoisomer (c) (80%), minor stereoisomer (e) (20%); $PEt_3$, cone angle 132°, (e) (50%), (h) (50%); $PPh_3$, cone angle 145°, (h) (67%), (e) (33%).

In the crystals of **(2)**, **(3)**, **(4)**, and **(11)** heb occurs as stereoisomer (a). For **(11)** the substituting ligand has a smaller effective size than might be anticipated as it adopts an orientation in which the mean plane through the four carbon atoms of the maleic anhydride makes a dihedral angle of 71.3° with the least-squares benzene ring plane. In **(11)** the heb accordingly occurs as stereoisomer (a). The stereochemistry of **(11)** is illustrated in Figure 2 and a detailed description of its crystal and molecular structure is given below.

One further general structural feature merits comment. We have postulated that eclipsing cannot take place over arene carbons bearing proximal methyl groups, and staggering is disallowed if any one of the bisected bonds is joined to a carbon atom bearing a proximal group.[1c] Hence when the heb is bound to a tripodal moiety, a single proximal methyl group is sufficient to ensure that the carbonyls eclipse the arene carbons. When all six methyls are distal as in (h), the staggered conformation expected from electronic considerations is adopted.

In the crystal of the mixed $C_5$–$C_6$ sandwich, **(12)**, the complexed heb occurs as stereoisomer (c) and a $\sigma_v$ plane of the $D_{5h}$ cyclopentadienyl ring coincides with the reflection plane of the $C_s$ heb.[2b] This arrangement presumably allows ethyl–ethyl and ethyl–cyclopentadienyl steric interactions to be minimised. The mean planes of the two rings are not parallel (dihedral angle 4°) and this has been attributed to the steric effects of the two proximal methyl groups.[2b] However, it should be noted that if the ring of higher rotational symmetry does not contain the rotational elements of the ring of lower symmetry, the mixed sandwich in consequence lacks overall rotational symmetry and there is no requirement that the rings be either planar and/or parallel. Thus in a mixed $C_6$–$C_5$ sandwich, even without substituents on either ring, it is not required that the rings be parallel and/or that the principal rotational axes of the individual rings be coextensive.

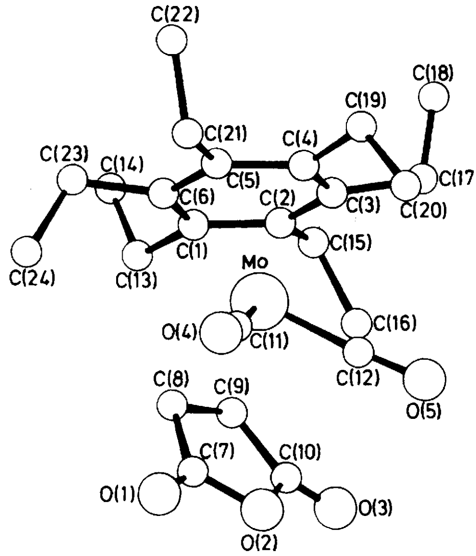

Figure 2. Molecular structure for **(11)**

The only other reported mixed $C_5$–$C_6$ sandwich of heb is the ruthenium congener of **(12)**, $[Ru(\eta^5\text{-}C_5H_5)(heb)]^+$ **(13)**.[3] No *X*-ray crystal structure is presently available for this compound but its low-temperature $^{13}C$ solution n.m.r. spectrum is consistent with the heb occurring as stereoisomer (a). In order to minimise steric interactions between the cyclopentadienyl ring and the proximal methyl groups, it is likely that this molecule adopts a lowest energy conformation in which a $\sigma_v$ plane of the cyclopentadienyl ring coincides with a $\sigma_d$ plane of the $D_{3d}$ heb ring (*i.e.* conformation type I of Astruc and co-workers[2b]).

*Stereodynamics of* ($\eta^6$-*Hexaethylbenzene*)*metal Complexes.*—Empirical force field calculations unequivocally show that uncorrelated ethyl group rotation leads to the lowest energy pathway for topomerisation in **(1)**, with a calculated barrier to the interconversion of stereoisomer (a) to stereoisomer (c) of 49.6 kJ $mol^{-1}$.[1b] All of the heb complexes so far examined show clear and unmistakable coalescence phenomena, involving only intramolecular exchange, occurring in their $^{13}C\text{-}\{^1H\}$ and/or $^{31}P\text{-}\{^1H\}$ solution n.m.r. spectra at low temperatures.* In the absence of significant intermolecular exchange processes, the observation of more than two resonances in the $^{31}P$ spectrum

---

* Site exchange processes involving arene–metal dissociation were ruled out by observation of separate resonances in a mixture of **(1)** and the transition metal complex at ambient temperature.

**Table 2.** Values for the free energies of activation of the interconversion reactions of the heb stereoisomers. All are $\Delta G^{\ddagger}_{200}$ (kJ mol$^{-1}$) except where noted

| Compound | (a) $\longrightarrow$ (c) | (c) $\longrightarrow$ (e) | (e) $\longrightarrow$ (h) | (h) $\longrightarrow$ (e) | (e) $\longrightarrow$ (c) | (c) $\longrightarrow$ (a) | (a1) $\rightleftharpoons$ (a2) |
|---|---|---|---|---|---|---|---|
| **(1)** | 49.6[a] | | | | | | |
| **(2)** | | | | | | | 48.3 ± 2.5[a–c] |
| **(3)** | | | | | | | 48.7 ± 0.8[a–c] |
| **(4)** | | 37.7 ± 2.0[b] | | | | | |
| **(5)** | 36.4 ± 2.0[d] | 33.5 ± 2.0[d] | 32.7 ± 1.3[d] | 35.2 ± 1.3[d] | 37.3 ± 2.0[d] | 34.3 ± 2.0[d] | |
| **(6)** | | | 35.2 ± 2.0[d] | 37.0 ± 2.0[d] | | | |
| **(7)** | | | 34.5 ± 2.5[d] | 37.1 ± 2.5[d] | | | |
| **(9)** | | 34.9 ± 1.5[d] | 34.9 ± 1.5[d] | 35.4 ± 1.5[d] | 39.1 ± 1.0[d] | | |
| **(11)** | 35.6 ± 2.0[b,e] | | | | | | |
| **(12)** | | 35.2 ± 1.7[b] | 36.8 ± 1.7[b] | 38.5 ± 1.7[b] | 36.4 ± 1.7[b] | | |
| **(13)** | | | | | | | 39.2 ± 1.2[b,f,g] |

[a] Calculated; see ref. 1*b*. [b] From $^{13}C-\{^1H\}$ spectrum. [c] $\Delta G^{\ddagger}_{300}$. [d] From $^{31}P-\{^1H\}$ spectrum. [e] From two-site exchange fitting for the carbonyl subspectrum; only tentatively assigned to (a) $\longrightarrow$ (c). [f] $\Delta G^{\ddagger}_{205}$. [g] Ref. 3.

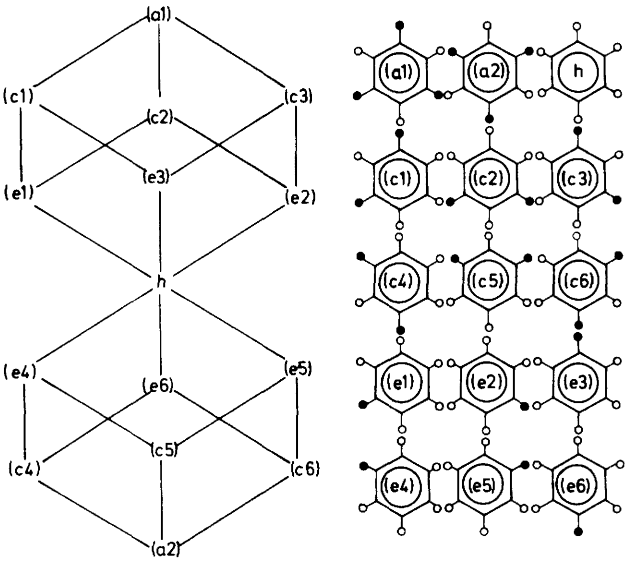

**Figure 3.** The 'Siamese cubes' interconversion scheme and the 15 'label' isomers of the four favoured stereoisomers for $[ML_3(heb)]$ complexes

of these complexes unequivocally demonstrates the presence of multiple heb stereoisomers in equilibrium in solution.* Such a situation applies for two of the complexes: $[Cr(CO)_2(PMe_3)(heb)]$, four resonances; $[Cr(CO)_2\{P(OPh)_3\}(heb)]$, three. Thus the almost isoenergetic nature of complexed heb stereoisomers is also well established in solution.

The interconversion of stereoisomers of heb occurs *via* ethyl group rotation and a general scheme, involving the four favoured stereoisomers, which allows not only stereoisomer interconversion but also topomerisation of the ethyl groups is illustrated in Figure 3. For heb bound to a rapidly rotating tripodal moiety there are a total of 15 individual 'label' isomers of the four favoured stereoisomers [two (a), six (c), six (e), one (h)]. Figure 3 shows the 15 label isomers arranged at the vertices of two cubes sharing a common vertex ('Siamese cubes') which is occupied by the unique label isomer (h). Any cube edge represents a single ethyl group rotation; a face diagonal, simultaneous double ethyl group rotation; a cube diagonal, simultaneous triple rotation. There are thus 105 possible first-order exchange reactions within the scheme, but if, by analogy with uncomplexed heb, only completely uncorrelated ethyl group rotation is significant, only the 24 exchanges represented by the edges of the two cubes will have effective rates. The rate constants for these exchanges can be separated into six groups; (a) $\longrightarrow$ (c), $k_1$; (c) $\longrightarrow$ (e), $k_2$; (e) $\longrightarrow$ (h), $k_3$; (h) $\longrightarrow$ (e), $k_4$; (e) $\longrightarrow$ (c), $k_5$; (c) $\longrightarrow$ (a), $k_6$. The pairs $k_1$ and $k_6$, $k_2$ and $k_5$, $k_3$ and $k_4$, are related by the relative populations of the exchanging label isomers.

This scheme successfully simulates the exchange-broadened $^{31}P-\{^1H\}$ and $^{13}C-\{^1H\}$ n.m.r. spectra of a number of heb complexes over a wide temperature range. We cannot, and do not, claim that the sets of $k$ values given in the Figure legends uniquely simulate the observed spectra, but from several hundred trial simulations in which were examined not only all possible permutations of the chemical shift assignments but also many variations of the three independent rate constant ratios, these parameters gave noticeably the best fit.

*Dicarbonyl*($\eta^6$-*hexaethylbenzene*)(*trimethylphosphine*)-*chromium*(0), **(5)**. This complex, with four resonances resolved in its low-temperature 145.79-MHz $^{31}P-\{^1H\}$ solution n.m.r. spectrum, perhaps best illustrates a general application of the Siamese cubes interconversion scheme. The four resonances, which coalesce to a sharp singlet with increasing temperature, show the presence of all four heb stereoisomers in equilibrium. The sequence in which the phosphorus atom visits each chemical environment is dependent on the ethyl group rotational sequence, and the $^{31}P$ spectrum therefore provides a probe of the ethyl group stereodynamics. As there is no unequivocal way of assigning an individual $^{31}P$ resonance to a given stereoisomer, spectral simulations were performed for all 24 possible permutations of the $^{31}P$ chemical shift assignments and that which gave noticeably the best fit shown is in Figure 4. It is of significance that for this complex the major stereoisomer of the crystal (c) is that least populated in $CD_2Cl_2$ solution at low temperatures. The free energies of activation at 200 K for the stereoisomer interconversion reactions are recorded in Table 2. These barriers are *ca.* 13 kJ mol$^{-1}$ lower than that calculated for the interconversion reaction (a) $\longrightarrow$ (c) in uncomplexed heb, and this not unexpected barrier lowering probably reflects higher ground-state energies resulting from increased non-bonding interactions in the stereoisomers of the complex.

The 90.1-MHz $^{13}C-\{^1H\}$ spectrum of **(5)** displays a reversible coalescence phenomenon in the carbonyl, arene, and alkyl sub-

---

* In the event of rapid rotation about the $\eta^6$-heb–metal bond, the observation of more than *one* resonance in the $^{31}P$ spectrum and/or the $^{13}C$ carbonyl subspectrum of these complexes demonstrates the presence of multiple heb stereoisomers in equilibrium in solution. However, it cannot be ruled out that this process may be slowed at low temperatures when resonances would be observed for the major rotamers of each heb stereoisomer [see Figure 6 for the situation with **(4)**].

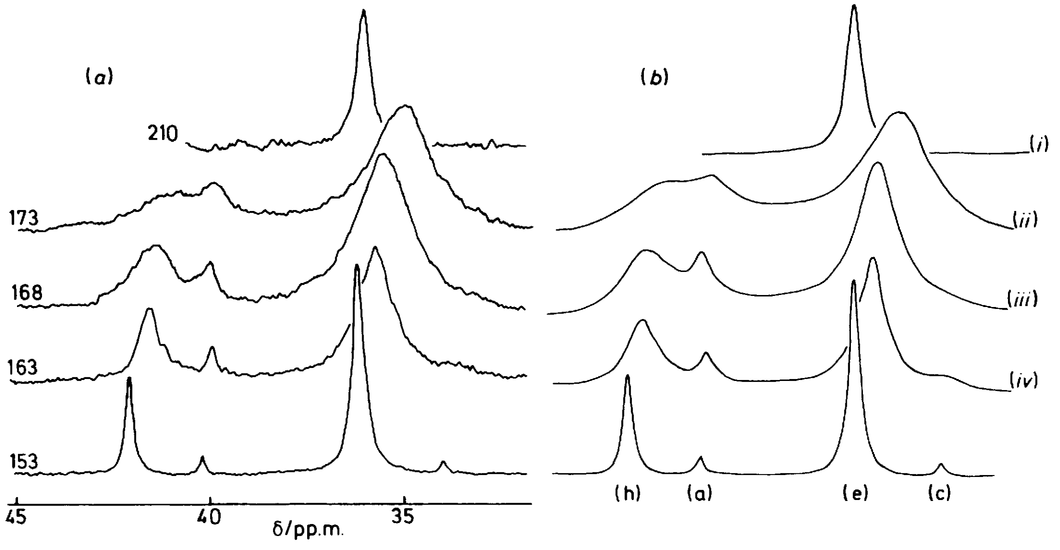

**Figure 4.** The variable-temperature (K) 145.79-MHz $^{31}P-\{^1H\}$ n.m.r. spectrum of (**5**) in $CD_2Cl_2$: (*a*) observed; (*b*) simulated. All 24 possible permutations of the chemical shift assignments to stereoisomers (a), (c), (e), and (h) were examined and that which gave the best fit is shown on the Figure. (*i*) $k_1 = 3\,000$, $k_2 = 20\,000$, $k_3 = 27\,000$, $k_4 = 6\,800$, $k_5 = 2\,000$, $k_6 = 12\,000$ $s^{-1}$; (*ii*) $k_1 = 90$, $k_2 = 600$, $k_3 = 800$, $k_4 = 200$, $k_5 = 60$, $k_6 = 360$ $s^{-1}$; (*iii*) $k_1 = 45$, $k_2 = 300$, $k_3 = 500$, $k_4 = 100$, $k_5 = 30$, $k_6 = 180$ $s^{-1}$; (*iv*) $k_1 = 7$, $k_2 = 175$, $k_3 = 200$, $k_4 = 55$, $k_5 = 13$, $k_6 = 21$ $s^{-1}$

spectra. At 153 K there are resolved two carbonyl-carbon resonances and numerous arene- and alkyl-carbon resonances.

*Dicarbonyl*(η$^6$-*hexaethylbenzene*)(*triethylphosphine*)-*chromium*(0), (**6**). Coalescence phenomena involving the arene and ethyl subspectra occur in the 90.1-MHz $^{13}C-\{^1H\}$ spectrum of (**6**) in $CD_2Cl_2$ solution at temperatures below 195 K. Four arene-carbon resonances are observed at 180 K and one of these (at 106 p.p.m.) is considerably broader and more intense than the other three. It seems likely that these resonances arise from the presence in equilibrium in solution of the two heb stereoisomers of the crystal, (e) and (h), with the broader signal attributable to (h).* The 145.79-MHz $^{31}P-\{^1H\}$ spectrum of (**6**) also displays a coalescence phenomenon with two resonances observed in the decoalesced spectrum. The downfield resonance is the rather more intense and, by comparison with the $^{13}C$ spectrum, is tentatively assigned to stereoisomer (h). The free energy of activation obtained from lineshape fitting studies of the $^{31}P$ spectrum is recorded in Table 2.

*Dicarbonyl*(η$^6$-*hexaethylbenzene*)(*triethylphosphine*)*molybdenum*(0), (**7**). Two resonances are observed in the decoalesced 145.79-MHz $^{31}P-\{^1H\}$ spectrum of (**7**). In this case the upfield resonance is the more intense and in the lineshape fitting studies was assigned to the heb stereoisomer (e); the downfield resonance was assigned to heb stereoisomer (h). The free energy of activation for the coalescence is recorded in Table 2.

*Dicarbonyl*(η$^6$-*hexaethylbenzene*)(*triphenyl phosphite*)-*chromium*(0), (**9**). Three resonances are observed in the low-temperature 145.79-MHz $^{31}P-\{^1H\}$ spectrum of this complex in $CD_2Cl_2$ solution. The Siamese cubes interconversion scheme gave excellent fit of calculated to observed spectra with the assignments to stereoisomers (c), (e), and (h) as shown in Figure 5. Thermodynamic parameters are recorded in Table 2.

Coalescence phenomena are observed in the arene and ethyl, but not the carbonyl, carbon subspectra. The resolution was too poor in the 90.1-MHz $^{13}C-\{^1H\}$ spectrum to undertake lineshape fitting.

*Dicarbonyl*(η$^6$-*hexaethylbenzene*)(*thiocarbonyl*)-*chromium*(0), (**4**). At 90.1-MHz, four $^{13}C$ resonances are observed at low temperature for each of the methyl- and arene-carbon subspectra of (**4**), indicating apparent $C_s$ symmetry for this molecule in $CD_2Cl_2$ solution. Such symmetry can conceivably arise from either, (*i*) (**4**) retaining in solution the heb stereoisomer of the crystal, (a), with arene–metal tripodal rotation slowed on the n.m.r. time-scale, or (*ii*) (**4**) adopting a different heb stereoisomer, (c) or (e), in solution and with rapid arene–metal tripodal rotation.

Interpretation (*i*) has been strongly advocated by McGlinchey *et al.*[2a,c] The evidence rests in part on the similarity of the $^{13}C$ solid-state and low-temperature solution n.m.r. spectra of (**4**). Of course, the interpretation of the solid-state spectrum should be based on the space group, $P2_1/c$, of the crystal of (**4**) and not on the point group, $C_s$ of the molecule. Since the molecule resides in a general position in the unit cell, all six arene carbons and all six ethyl groups of the molecule should be chemically inequivalent. However, possibly as the result of accidental isochronies, only four arene-, three methylene-, and three methyl-carbon resonances are observed, and the evidence for similar solution and solid-state structures for (**4**) is therefore not strictly comparable to that cited for the 2-hydroxyhomotropylium cation, where all eight carbon atoms of the molecule are observed to be chemically inequivalent both in solution and in the crystal unit cell.[7]

An additional argument is based on the assignment of chemical shifts within the $^{13}C$ low-temperature solution alkyl and arene subspectra.[2c] In essence, the chemical shift differences within the alkyl-carbon subspectrum result from differences in the proximal or distal methyl environments, and within the arene carbon subspectrum, depend on whether the ring carbons bear proximal or distal methyl groups. The assignment of individual resonances is by comparison with the solution spectrum of (**8**) where all the methyl groups are distal. This argument, particularly for the $^{13}C$-ethyl resonances, where distal methyls would absorb in the range 13—16 p.p.m. and proximal methyls in the range 18—25 p.p.m., is straightforward and appealing in its simplicity. Thus it appears that the low-temperature $^{13}C$ spectrum of (**4**) shows three carbons in the proximal range and three in the distal range for the methyl-,

---

* Trial simulations were performed by assigning arbitrary chemical shift values to the fourth, unobserved arene-carbon resonance of stereoisomer (e). The resonance assigned to stereoisomer (h) always appeared broader than the others at intermediate rates of exchange.

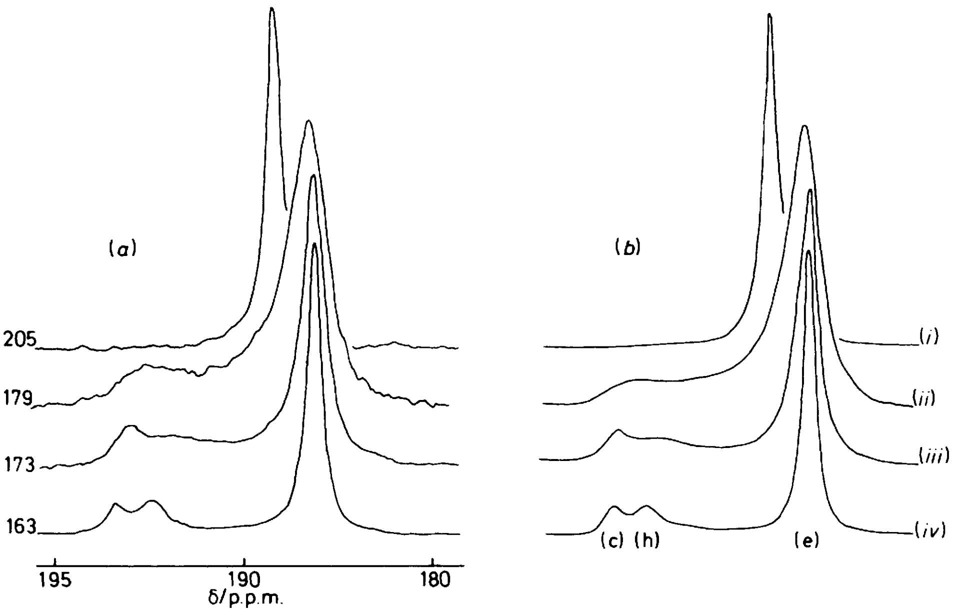

**Figure 5.** The variable-temperature (K) 145.79 MHz $^{31}P-\{^1H\}$ n.m.r. spectrum of (**9**) in $CD_2Cl_2$: (*a*) observed; (*b*) simulated. All six possible permutations of the chemical shift assignments to stereoisomers (c), (e), and (h) were examined and that which gave the best fit is shown. (*i*) $k_2 = 4\,500$, $k_3 = 4\,500$, $k_4 = 3\,600$, $k_5 = 450$ s$^{-1}$; (*ii*) $k_2 = 420$, $k_3 = 420$, $k_4 = 336$, $k_5 = 42$ s$^{-1}$; (*iii*) $k_2 = 200$, $k_3 = 200$, $k_4 = 160$, $k_5 = 20$ s$^{-1}$; (*iv*) $k_2 = 50$, $k_3 = 50$, $k_4 = 40$, $k_5 = 5$ s$^{-1}$

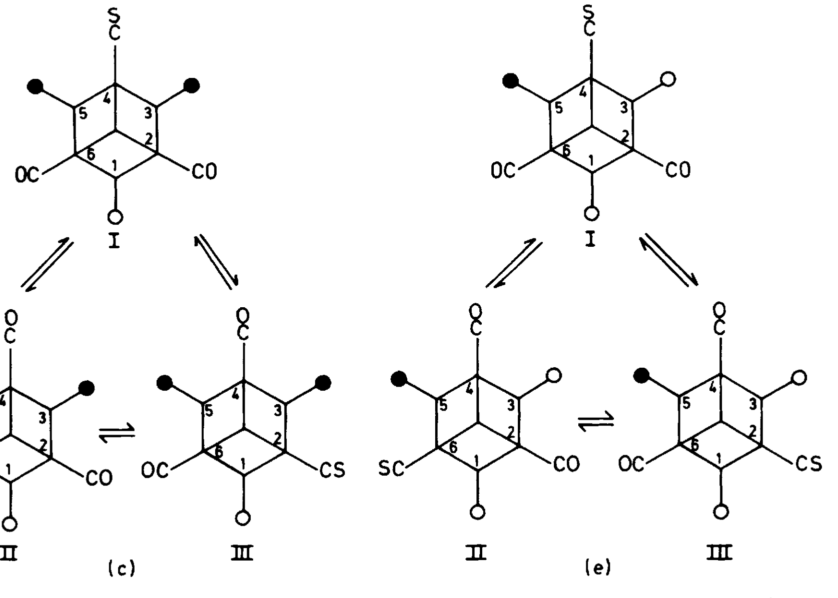

**Figure 6.** The three most highly populated rotamers for heb stereoisomers (c) and (e) obtained by rotation about the $\eta^6$-heb–chromium bond in (**4**)

methylene-, and ring-carbon environments. Hence it follows that (**4**) adopts the same structure in solution as in the crystal, *i.e.* heb stereoisomer (a).

However, while it is reasonable to assume some proximal–distal contribution to the chemical shift differences within a subspectrum, it is not at all clear that this is the only, nor indeed perhaps the major, contribution and the simple proximity argument fails when the chemical shift differences observed for the methylene and arene carbons are considered. Only very small chemical shift differences should be expected for the methylene carbon signals since these atoms all have similar proximities to the chromium. The same applies to the arene carbons. McGlinchey's argument thus critically hinges on the assignment of the individual methyl carbon resonances in the range 13—16 p.p.m. to only distal, and those in the range 18—25 p.p.m. to only proximal environments.

There is moreover an alternative plausible explanation for the chemical shift differences within a given subspectrum, which requires the assumption of a heb stereoisomer with $C_s$ symmetry, but which does not of necessity require slowed arene–metal tripodal rotation. We consider it possible that the chemical shift differences may to a substantial extent also depend on whether or not the carbons (methyl, methylene, and arene) are eclipsed by the tripodal ligands in the most highly populated rotamers. This is exemplified in Figure 6 for stereoisomers (c) and (e) of (**4**). The chemical shifts $\nu_n$(av) of carbons n

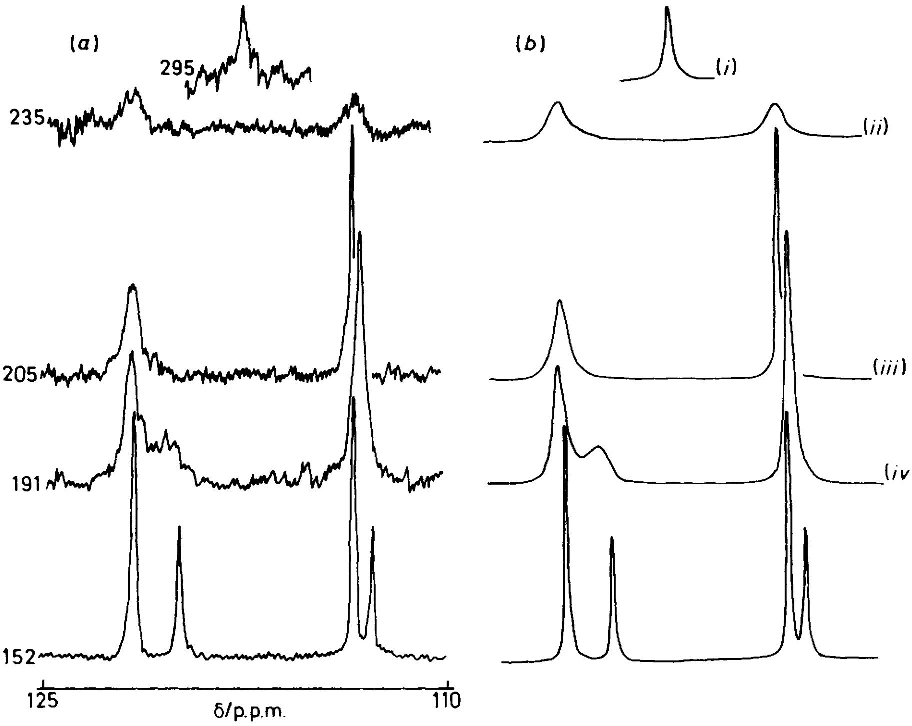

**Figure 7.** The variable-temperature 90.1-MHz $^{13}C-\{^1H\}$ n.m.r. subspectrum of the arene carbon atoms of (**4**) in $CD_2Cl_2$; (*a*) observed; (*b*) simulated. (*i*) $k_2 = 700\,000\ s^{-1}$; (*ii*) $k_2 = 40\,000\ s^{-1}$; (*iii*) $k_2 = 1\,000\ s^{-1}$; (*iv*) $k_2 = 200\ s^{-1}$

(arene, methylene, or methyl), averaged by rapid rotation about the $\eta^6$-heb–metal bond, are given below where $x_N$ is the mole fraction of rotamer N (Figure 6) and $\nu_n^N$ is the chemical shift of carbon n in rotamer N. Except for accidental isochronies, both

For stereoisomer (c)

$$x_I \neq x_{II} = x_{III}$$

$$\begin{aligned}
\nu_1(av) &= x_I\nu_1^{I} + 2x_{II}\nu_1^{II}\\
\nu_2(av) &= x_I\nu_2^{I} + x_{II}(\nu_2^{II} + \nu_6^{II})\\
\nu_3(av) &= x_I\nu_3^{I} + x_{II}(\nu_3^{II} + \nu_3^{III})\\
\nu_4(av) &= x_I\nu_4^{I} + 2x_{II}\nu_4^{II}\\
\nu_5(av) &= x_I\nu_2^{I} + x_{II}(\nu_3^{III} + \nu_3^{II})\\
\nu_6(av) &= x_I\nu_2^{I} + x_{II}(\nu_2^{III} + \nu_6^{III})
\end{aligned}$$

$$\underbrace{\nu_2(av) = \nu_6(av) \neq \nu_4(av)}_{\text{eclipsed}} \neq \nu_1(av) \neq \nu_3(av) = \nu_5(av)$$

For stereoisomer (e)

$$x_I = x_{II} \neq x_{III}$$

$$\begin{aligned}
\nu_1(av) &= x_I(\nu_1^{I} + \nu_1^{II}) + x_{III}\nu_1^{III}\\
\nu_2(av) &= 2x_I\nu_2^{I} + x_{III}\nu_2^{III}\\
\nu_3(av) &= x_I(\nu_1^{I} + \nu_1^{II}) + x_{III}\nu_1^{III}\\
\nu_4(av) &= x_I(\nu_4^{I} + \nu_4^{II}) + x_{III}\nu_4^{III}\\
\nu_5(av) &= 2x_I\nu_5^{I} + x_{III}\nu_5^{III}\\
\nu_6(av) &= x_I(\nu_4^{I} + \nu_4^{II}) + x_{III}\nu_4^{III}
\end{aligned}$$

$$\underbrace{\nu_2(av) \neq \nu_4(av) = \nu_6(av)}_{\text{eclipsed}} \neq \nu_1(av) \neq \nu_3(av) \neq \nu_5(av)$$

examples should give rise to four resonances for each of the methyl, methylene, and arene subspectra, and there is no obvious requirement that chemical shift differences within an individual subspectrum should be very different for methyl, methylene, or arene carbons. The four lines in each subspectrum should then be separated into two groups of two adjacent lines of relative intensities approximately 2:1 as observed.

If the above argument is correct, then it also follows that assignments to distal environments based purely on the arene and alkyl carbon chemical shifts, observed in the solution spectrum of (**8**) become suspect, as the structure adopted by the six most highly populated rotamers of this complex is likely to be dictated by electronic rather than steric considerations, and hence will be similar to that observed in the crystal where the projections of the tripodal ligands bisect the carbon–carbon bonds of the arene.[1a,b] Despite the all-distal methyl group arrangement for (**8**), it is noteworthy that in the arene subspectrum of its $^{13}C$ solid-state n.m.r. spectrum, there are five well-resolved resonances, with chemical shifts ranging from 104.5 to 114.6 p.p.m.[1b,*]

In order to test the alternative explanation, spectral simulations based on interpretation (*ii*) (above) were attempted.

The arene subspectrum of the $^{13}C-\{^1H\}$ solution spectrum of (**4**) was simulated over the temperature range 152—295 K using the Siamese cubes exchange scheme. Excellent fit of simulated on observed spectra (Figure 7) was obtained by assuming that the heb stereoisomer of the crystal, (a), was not retained in solution and the four resonances observed at 152 K were assigned to the six label isomers of stereoisomer (c). Allowing heb stereoisomer interconversion to occur only by single ethyl group rotation requires the assumption of low intensity unobserved resonances for the six label isomers of stereoisomers (e) and for the unique label isomer of stereoisomer (h). Provided that the assumed populations of (e) and (h) do not exceed about

---

[*] Although two heb stereoisomers, (h) (67%) and (e) (33%) are found in the crystal of (**8**), in its solid-state $^{13}C$ n.m.r. spectrum the resonances of the minor stereoisomer are overlapped and obscured by those of the major stereoisomer.

5% of that of (c), the chemical shifts and intensities actually assigned to the unobserved resonances are unimportant to the appearance of the simulated exchange-broadened spectrum. In the interconversion scheme the two vertices corresponding to the label isomers of stereoisomers (a) were removed from the Siamese cubes. As resonances were not observed for stereoisomers (e) and (h), only the activation parameter obtained for uncorrelated ethyl group rotation in (c) can be considered meaningful, and is recorded in Table 2.

*Dicarbonyl*($\eta^6$-*hexaethylbenzene*)($\eta^2$-*maleic anhydride*)-*chromium*(0), **(10)**. A coalescence phenomenon is observed in the arene carbon subspectrum of the 90.1-MHz $^{13}C$ spectrum of **(10)** and at 153 K in $CD_2Cl_2$ solution three broad resonances are observed. The carbonyl-carbon subspectrum merely broadens and no decoalescence is observed at the lowest accessible temperature in this solvent. No lineshape fitting was attempted for this compound.

*Dicarbonyl*($\eta^6$-*hexaethylbenzene*)($\eta^2$-*maleic anhydride*)-*molybdenum*(0), **(11)**. Coalescence phenomena involving all the subspectra occur in the 90.1-MHz $^{13}C$ spectrum of **(11)** in $CD_2Cl_2$–$CDFCl_2$ at temperatures below 180 K. In the decoalesced spectrum, two carbonyl resonances are observed, with some asymmetry on the upfield resonance, showing that there are at least two, and possibly more, heb stereoisomers present. The arene-carbon resonances are to some extent obscured by solvent resonances, and it is not possible to observe their number in the decoalesced subspectrum and hence make reasonable assignments to heb stereoisomers. Lineshape fitting was therefore limited to simulation of simple two-site exchange involving the carbonyl resonances.

($\eta^5$-*Cyclopentadienyl*)($\eta^6$-*hexaethylbenzene*)*iron*(II) *hexafluorophosphate*, **(12)**. It has previously been reported that the dynamic behaviour of the ethyls in **(12)** involves a facile interconversion of the proximal and distal methyl groups, and hence that this rotation is not slow on the n.m.r. time-scale even at 153 K on a 400-MHz spectrometer.[2a,b] It is therefore difficult to reconcile these reports with our observation, using a 360-MHz spectrometer, of coalescence phenomena occurring in all of the carbon subspectra of this compound in $CHFCl_2$ or $CD_2Cl_2$ solutions at temperatures below 160 K. In particular, the coalescence phenomenon occurring in the cyclopentadienyl-carbon subspectrum is well defined and three resonances are observed in $CHFCl_2$ solution at 140 K. At this temperature, the arene and ethyl subspectra are also multiply split, although not apparently fully decoalesced.

Tripling of the cyclopentadienyl resonance can conceivably arise from the slowing, either individually or jointly, of the two major intramolecular rotational processes: rotation of the ethyl groups about the arene; rotation of the two cyclic moieties relative to each other. To interpret the slow-exchange limit cyclopentadienyl-carbon subspectrum, the two general cases, (A) and (B), were subjected to detailed analysis, similar to that described above for **(4)**.

For case (A), the presence in solution of only one heb stereoisomer of $C_s$ symmetry is assumed. (*i*) Both rotations are slow on the n.m.r. time-scale. The molecule has overall $C_s$ symmetry and three cyclopentadienyl-carbon resonances are expected. (*ii*) Rotation of the ethyl groups is slow, but rotation of the cyclic moieties is rapid. Only one resonance is expected for the cyclopentadienyl-carbon subspectrum. (*iii*) Ethyl group rotation is rapid, but rotation of the cyclic moieties is slow, although some slight displacement of the rings relative to each other is allowed to permit retention of the most favoured conformation for each of the label isomers. Ethyl group rotation causes a topomerisation within the heb moiety, one effect of which will be a pseudorotation of the arene relative to the cyclopentadienyl ring. All of the cyclopentadienyl carbons thus become chemically equivalent.

**Table 3.** Low-temperature n.m.r. chemical shifts for the moiety subspectra used in the lineshape fitting studies

| Compd. | Solvent | $T$/K | Nucleus | Moiety | Subspectral chemical shifts (δ/p.p.m.)[a] |
|---|---|---|---|---|---|
| **(2)**[b] | $CD_2Cl_2$ | 202 | $^{13}C-\{^1H\}$ | $C_{arene}$ | 108.8, 117.2 |
| **(3)**[b] | $CD_2Cl_2$ | 206 | $^{13}C-\{^1H\}$ | $C_{arene}$ | 114.7, 121.6 |
| **(4)**[c] | $CD_2Cl_2$ | 163 | $^{13}C-\{^1H\}$ | $C_{arene}$ | 112.8, 113.8, 119.9, 121.7 |
| **(5)**[c] | $CD_2Cl_2$ | 163 | $^{31}P-\{^1H\}$ | $PMe_3$ | 33.8, 35.8, 40.0, 41.6 |
| **(6)**[c] | $CD_2Cl_2$ | 153 | $^{31}P-\{^1H\}$ | $PEt_3$ | 67.5, 68.9 |
| **(7)**[c] | $CD_2Cl_2$ | 168 | $^{31}P-\{^1H\}$ | $PEt_3$ | 42.6, 46.9 |
| **(9)**[c] | $CD_2Cl_2$ | 163 | $^{31}P-\{^1H\}$ | $P(OPh)_3$ | 188.2, 192.7, 193.5 |
| **(11)**[c] | $CD_2Cl_2$ | 148 | $^{13}C-\{^1H\}$ | CO | 235.1, 236.3 |
| **(12)**[c] | $CHFCl_2$ | 140 | $^{13}C-\{^1H\}$ | $C_5H_5$ | 76.8, 77.6, 78.2 |

[a] Chemical shifts are in p.p.m. downfield from $SiMe_4$ ($^{13}C-\{^1H\}$) or from $H_3PO_4$ ($^{31}P-\{^1H\}$). [b] Ref. 1*b*. [c] This work.

For case (B) relative rotation of the cyclic moieties is rapid, ethyl group rotation is slow and three heb stereoisomers coexist in n.m.r.-detectable concentrations. It seems plausible that structural criteria similar to those previously established[1c] to predict relative stereoisomer stability for heb bound to tripodal moieties can be similarly applied to **(12)**. For this complex, stereoisomer (a) becomes disfavoured on steric grounds, thus leaving (c), (e), and (h) as the most favoured in solution. The cyclopentadienyl carbons of a given heb stereoisomer are chemically equivalent and three resonances are seen.

Only cases A(*i*) and (B) are consistent with the observed slow-exchange cyclopentadienyl-carbon subspectrum, and lineshape fitting studies were performed using these as the bases for exchange-broadening. In these studies, all possible permutations of the $^{13}C$ chemical shift assignments were examined.

For case A(*i*), exchange-broadening could arise from the onset of rapid rotation of either the ethyl groups or of one of the cyclic moieties. For the former, spectral simulation was attempted using the Siamese cubes exchange scheme. Assuming that only heb stereoisomer (c) was present in n.m.r.-observable concentration, calculations were performed in a similar manner to those described for the arene carbon subspectrum of **(4)**. However, in this instance, the fit of simulated to observed spectra was unacceptably poor.

The number of equivalent major low-energy rotamers resulting from rotations about the metal is equal to the product of the orders of the principal rotational axes of the individual cyclic moieties (Figure 8). Hence a five-site exchange scheme was used to simulate the spectral effect of the onset of rapid relative rotation of the cyclic moieties. Not even a remotely good fit of calculated to observed spectra was obtained, and we conclude therefore that, as might be expected, relative rotation of the cyclic moieties remains rapid at the lowest observed temperature, 140 K.

For case (B) the three resonances observed in the decoalesced cyclopentadienyl-carbon subspectrum were assigned to stereoisomers (c), (e), and (h). The Siamese cubes interconversion scheme, with the two vertices representing the label isomers of stereoisomer (a) removed, was used to simulate the exchange-broadened spectrum. Excellent fit of the calculated to the observed spectrum was obtained using the chemical shift assignments shown in Figure 9. Thermodynamic parameters are recorded in Table 2.

Although we consider that for **(12)** stereoisomer (a) is disfavoured on steric grounds, the low-temperature $^{13}C$ spectrum recently reported by Green and co-workers[3] for **(13)** is consistent with the presence of only this stereoisomer in solution. This difference from **(12)** has been attributed[3] to the greater size

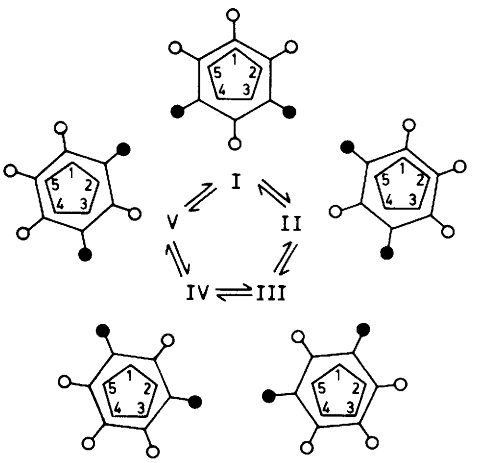

**Figure 8.** The five most highly populated rotamers obtained from rotation about the iron atom of the cyclic moieties in (**12**)

of a ruthenium atom which allows a reduction in the repulsive interactions between the cyclopentadienyl moiety and the proximal methyl groups. A coalescence phenomenon attributed to the onset of rapid ethyl group rotation has been observed in the $^{13}C$ spectrum of (**13**).[3] Different linewidths are seen for each of the two resonances of the arene-carbon subspectrum at a given temperature within the range appropriate to intermediate rates of exchange.† We consider that the differing $T_2$* values are likely to be a manifestation of ethyl group rotation occurring *via* the series of other stereoisomers whose populations are too low to be n.m.r. observable.

As noted above, in a mixed sandwich of this type there is no requirement that the rings be parallel and/or that the principal rotational axes of the individual rings be co-extensive. For (**13**) there are 15 equivalent major low-energy rotamers resulting from rotations about the ruthenium. In the event that the rate for the relative rotation of the cyclic moieties can be brought within the n.m.r. time-scale, subspectra consistent with $C_s$ symmetry will be observed for cyclopentadienyl, arene, and ethyl carbons. Such is not the case, and we conclude that as for (**12**), cyclic moiety rotation about the metal remains rapid down to 140 K.

*Concluding Remarks.*—We have shown that with the exception of (**8**), all the ($\eta^6$-heb)metal complexes so far examined display coalescence phenomena in their variable-temperature n.m.r. spectra that can be attributed to the onset of uncorrelated rapid rotation of the ethyl groups about the benzene ring. We have also adduced unequivocal evidence that for a number of the complexes, heb stereoisomers coexist in equilibrium in solution and that the relative energies of the favoured stereoisomers span a much smaller range than that calculated for (**1**) itself.[1b] In light of these finding, the case of (**4**) acquires special significance. Obviously, McGlinchey's arguments[2a,c] for hindered rotation about the arene–chromium bond of (**4**) cannot easily be dismissed, but nor can the alternative interpretation of the same observations that we have attempted to develop in this paper. In support of our own arguments we cite the facts, first, that for all the heb complexes so far examined, including (**4**), the n.m.r. spectra can be satisfactorily analysed wholly on the basis of hindered rotation about the ethyl–arene bond. An analogous situation has recently been reported for dicarbonyl(1,4-di-t-butyl-2-methoxybenzene)(triphenylphosphine)chromium(0), where, despite an energy maximum for arene–chromium rotation corresponding to movement of triphenylphosphine past a t-butyl group, the spectra are best interpreted by invoking hindered rotation of the methoxy group about the arene–oxygen bond.[8] Second, our lineshape fitting studies have established that the heb stereoisomers of the crystal need not necessarily be those most favoured in solution. Therefore any interpretation of the n.m.r. spectra of these complexes must allow for this possibility, although for all cases except (**4**), satisfactory fit of calculated to observed spectra can be achieved by assigning some of the spectral lines to the stereoisomers seen in the crystal. Finally, it is generally believed that in the absence of quite exceptional electronic and/or steric factors, the barrier to rotation about a $\eta^6$-arene–metal bond is too small to allow this process to be observed on the n.m.r. time-scale.[9] The burden of proof that such rotation has indeed been slowed therefore demands evidence that admits of no other reasonable alternative explanation.

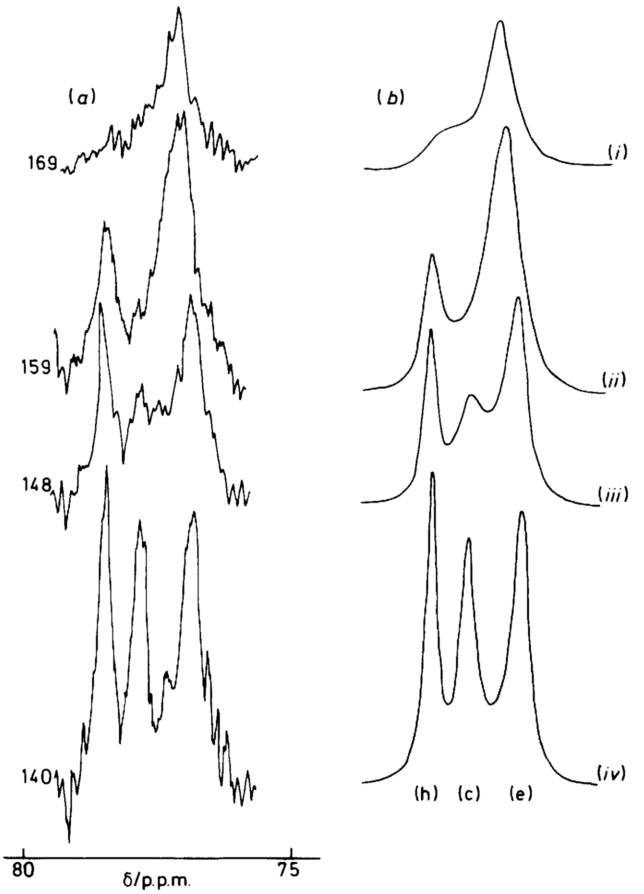

**Figure 9.** The variable-temperature (K) 90.1-MHz $^{13}C-\{^1H\}$ n.m.r. subspectrum of the arene carbon atoms of (**12**) in $CD_2Cl_2$: (*a*) observed; (*b*) simulated. (*i*) $k_2 = 300, k_3 = 100, k_4 = 30, k_5 = 160\ s^{-1}$; (*ii*) $k_2 = 120, k_3 = 40, k_4 = 13, k_5 = 75\ s^{-1}$; (*iii*) $k_2 = 55, k_3 = 18, k_4 = 6, k_5 = 30\ s^{-1}$; (*iv*) $k_2 = 25, k_3 = 8, k_4 = 3, k_5 = 15\ s^{-1}$

In our view, the issue must be considered unsettled, and the definitive resolution of this problem must await further evidence of an experimental or a theoretical nature.

*Structure of Dicarbonyl*($\eta^6$-*hexaethylbenzene*)($\eta^2$-*maleic anhydride*)*molybdenum*(0), (**11**).—A literature search reveals crystal and molecular structures for only two other compounds in which the maleic anhydride acts as a unidentate, dihapto

---

† We thank Dr. Green for providing these spectra prior to publication.

**Table 4.** Selected bond distances (Å) and bond angles (°) for **(11)**

| | | | | | | | |
|---|---|---|---|---|---|---|---|
| Mo–C(1) | 2.409(13) | C(4)–C(5) | 1.445(20) | C(6)–C(1)–C(2) | 119.2(1.2) | O(2)–C(7)–O(1) | 118.1(1.6) |
| Mo–C(2) | 2.422(12) | C(5)–C(6) | 1.432(19) | C(1)–C(2)–C(3) | 120.1(1.2) | C(7)–O(2)–C(10) | 107.8(1.3) |
| Mo–C(3) | 2.410(13) | C(6)–C(1) | 1.419(19) | C(2)–C(3)–C(4) | 121.1(1.1) | Mo–C(11)–O(4) | 172.6(1.4) |
| Mo–C(4) | 2.386(12) | C(8)–C(9) | 1.485(22) | C(3)–C(4)–C(5) | 119.2(1.2) | Mo–C(12)–O(5) | 175.9(1.4) |
| Mo–C(5) | 2.430(13) | C(7)–C(8) | 1.446(22) | C(4)–C(5)–C(6) | 119.2(1.3) | C(11)–Mo–C(12) | 87.8(0.6) |
| Mo–C(6) | 2.458(13) | C(9)–C(10) | 1.433(21) | C(5)–C(6)–C(1) | 120.9(1.2) | C(8)–Mo–C(11) | 76.5(0.6) |
| Mo–C(8) | 2.284(14) | C(7)–O(2) | 1.363(19) | O(1)–C(7)–C(8) | 129.6(1.7) | C(9)–Mo–C(12) | 85.7(0.6) |
| Mo–C(9) | 2.282(15) | C(10)–O(2) | 1.426(19) | C(7)–C(8)–C(9) | 103.6(1.3) | C(8)–Mo–C(9) | 38.0(0.6) |
| Mo–C(11) | 1.912(15) | C(7)–O(1) | 1.217(20) | C(8)–C(9)–C(10) | 107.4(1.3) | Mo–C(8)–C(9) | 70.9(0.8) |
| Mo–C(12) | 1.888(16) | C(10)–O(3) | 1.142(22) | C(9)–C(10)–O(3) | 129.7(1.6) | Mo–C(9)–C(8) | 71.1(0.8) |
| C(1)–C(2) | 1.451(19) | C(11)–O(4) | 1.177(19) | C(9)–C(10)–O(2) | 108.6(1.5) | Mo–C(8)–C(7) | 112.5(1.0) |
| C(2)–C(3) | 1.401(19) | C(12)–O(5) | 1.171(19) | O(2)–C(10)–O(3) | 121.5(1.5) | Mo–C(9)–C(10) | 112.4(1.1) |
| C(3)–C(4) | 1.437(16) | | | C(8)–C(7)–O(2) | 112.3(1.4) | | |

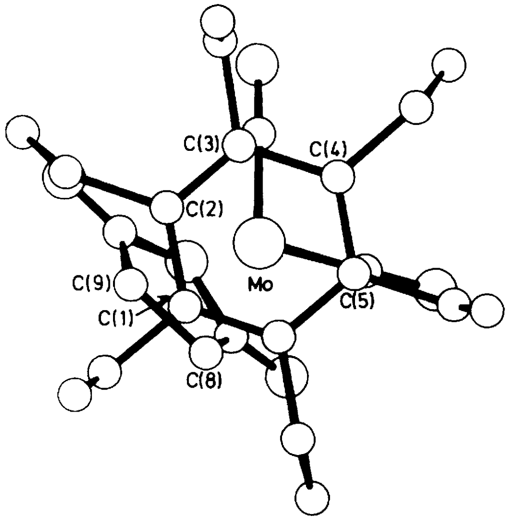

**Figure 10.** The molecular structure of **(11)** viewed along the normal to the least-squares benzene ring plane

**Table 5.** Deviations (Å) from the mean planes * of the cyclic moieties in **(11)**

| Atom | Plane A: C(1),C(2),C(3),-C(4),C(5),C(6) | Plane B: Mo,C(8),C(9) | Plane C: O(1),O(2),O(3),-C(7),C(8),C(9),C(10) |
|---|---|---|---|
| Mo | 1.9509 | 0.0000 | 2.0433 |
| O(1) | 5.4644 | 1.8128 | −0.0591 |
| O(2) | 5.2875 | 2.1120 | 0.1005 |
| O(3) | 4.6001 | 1.6724 | −0.0811 |
| O(4) | 3.5552 | 1.6884 | 2.8101 |
| O(5) | 3.5756 | 2.6700 | 3.2298 |
| C(1) | 0.0344 | −2.3656 | 1.2761 |
| C(2) | −0.0106 | −1.7093 | 2.0479 |
| C(3) | −0.0195 | −0.8765 | 3.3756 |
| C(4) | 0.0261 | −0.6474 | 3.9929 |
| C(5) | −0.0026 | −1.3540 | 3.2553 |
| C(6) | −0.0278 | −2.2296 | 1.9102 |
| C(7) | 4.7638 | 1.3253 | −0.0042 |
| C(8) | 3.3947 | 0.0000 | 0.0011 |
| C(9) | 3.1391 | 0.0000 | 0.0096 |
| C(10) | 4.3334 | 1.2982 | 0.0332 |
| C(11) | 3.0245 | 1.0920 | 2.4590 |
| C(12) | 2.9971 | 1.6654 | 2.7408 |
| C(13) | 0.0205 | −3.2704 | −0.1389 |
| C(14) | −1.4278 | −4.7194 | −0.1958 |
| C(15) | −0.2251 | −2.0510 | 1.4807 |
| C(16) | 1.0469 | −0.9413 | 1.0426 |
| C(17) | −0.2432 | −0.3212 | 4.2543 |
| C(18) | −1.7438 | −1.3429 | 4.8867 |
| C(19) | −0.0892 | 0.1768 | 5.4713 |
| C(20) | 1.2199 | 1.7015 | 5.8129 |
| C(21) | 0.0081 | −1.1422 | 3.9150 |
| C(22) | −1.5270 | −2.2349 | 4.6601 |
| C(23) | −0.2635 | −3.1260 | 1.2072 |
| C(24) | 1.0422 | −2.5078 | 0.3729 |

* Angles between normals to the planes are: AB, 39.3; AC, 108.7; BC, 70.7°.

ligand:* dicarbonyl($\eta^2$-maleic anhydride)($\eta^6$-mesitylene)-chromium(0), **(14)**,[11] and ($\eta^2$-maleic anhydride)tris(trimethyl phosphite)cobalt(0).[12] While the structure of **(11)** is generally similar to that of **(14)**, there are also marked differences. The geometry at the Mo atom more closely reflects octahedral co-ordination and the OC–Mo–CO bond angle of 87.8° [81.8° for **(14)**][11] is quite close to the ideal value of 90°. The arene ring is planar (the maximum deviation of the individual arene carbon atoms from the mean ring plane does not exceed 0.034 Å), the individual C–C (arene) bond lengths are within the normal range and there is no bond length alternation. The Mo atom is symmetrically bonded to both the arene and the maleic anhydride [Mo–C(8) 2.284(14), Mo–C(9) 2.282(15) Å] although the double bond of the latter moiety is inclined to the arene ring plane at an angle of 9.9° [1.3° in **(14)**].[11] This inclination, however, may be due less to intramolecular effects than to intermolecular interactions between one of the maleic anhydride carbonyl oxygens and a distal methyl group of an adjacent molecule in the unit cell.

The double bond length C(8)–C(9) of 1.485 Å [1.463 Å in **(14)**][11] is considerably greater than that of non-co-ordinated maleic anhydride (1.337 Å) and this can be attributed to the back donation contribution to the metal–ligand interaction. The co-ordinated maleic anhydride is not planar as the ring oxygen is displaced by 0.10 Å [0.09 Å in **(14)**][11] from the average plane of the four ring carbon atoms. The dihedral angle between this plane and the mean plane is 71.3° [69.6° in **(14)**].[11] The relative orientation of the arene and the other three ligands in **(14)** corresponds to a conformation intermediate between staggered and eclipsed. In **(11)**, however, the carbonyls efficiently eclipse the arene carbons to which the distal ethyl groups are attached, demonstrating once again that in [$ML_3$(heb)] complexes it is steric rather than electronic effects which determine the orientation of the tripod with respect to the arene.

---

* There is also a report[10] of maleic anhydride acting as a bridging ligand between the two iron atoms in hexacarbonyl-μ-(3,6-diphenyl-pyridazine)-(maleic anhydride)di-iron.

**Table 6.** Atomic parameters for (**11**)

| Atom | *x* | *y* | *z* |
|---|---|---|---|
| Mo | 0.227 9(1) | 0.250 0(1) | 0.189 8(1) |
| O(1) | 0.413 9(9) | 0.121 9(11) | 0.386 0(18) |
| O(2) | 0.440 1(7) | 0.230 7(7) | 0.228 5(13) |
| O(3) | 0.444 5(11) | 0.310 0(11) | 0.017 6(19) |
| O(4) | 0.256 7(9) | 0.205 5(10) | 0.520 2(17) |
| O(5) | 0.321 2(9) | 0.420 1(10) | 0.259 3(17) |
| C(1) | 0.145 3(8) | 0.185 9(9) | −0.003 8(16) |
| C(2) | 0.150 3(7) | 0.280 0(8) | −0.033 9(15) |
| C(3) | 0.125 1(8) | 0.341 0(9) | 0.074 0(17) |
| C(4) | 0.094 7(8) | 0.312 1(9) | 0.215 8(16) |
| C(5) | 0.085 4(9) | 0.218 6(9) | 0.243 5(17) |
| C(6) | 0.109 3(8) | 0.156 7(9) | 0.131 2(16) |
| C(7) | 0.394 3(11) | 0.160 1(11) | 0.272 3(20) |
| C(8) | 0.326 5(9) | 0.143 6(10) | 0.173 3(16) |
| C(9) | 0.338 5(9) | 0.208 9(10) | 0.051 9(18) |
| C(10) | 0.410 0(9) | 0.259 4(15) | 0.087 6(18) |
| C(11) | 0.251 4(9) | 0.222 4(10) | 0.392 8(18) |
| C(12) | 0.288 0(10) | 0.353 2(11) | 0.234 1(19) |
| C(13) | 0.171 5(9) | 0.122 1(10) | −0.122 9(18) |
| C(14) | 0.100 1(9) | 0.099 8(10) | −0.229 5(18) |
| C(15) | 0.173 4(9) | 0.314 6(10) | −0.192 2(19) |
| C(16) | 0.260 2(12) | 0.352 8(14) | −0.200 9(24) |
| C(17) | 0.119 8(9) | 0.439 1(10) | 0.037 8(18) |
| C(18) | 0.037 2(10) | 0.459 4(11) | −0.034 0(19) |
| C(19) | 0.0614(9) | 0.378 5(10) | 0.328 8(18) |
| C(20) | 0.123 7(12) | 0.420 7(14) | 0.435 6(25) |
| C(21) | 0.0514(8) | 0.188 3(9) | 0.390 7(17) |
| C(22) | −0.046 2(12) | 0.182 8(13) | 0.372 2(21) |
| C(23) | 0.088 0(9) | 0.059 2(10) | 0.151 3(18) |
| C(24) | 0.155 9(10) | 0.003 0(11) | 0.229 2(20) |

## Experimental

*Synthesis.—Tricarbonyl*($\eta^6$*-hexaethylbenzene*)*chromium*(0), (**2**), *and tricarbonyl*($\eta^6$*-hexaethylbenzene*)*molybdenum*(0), (**3**). These were prepared as previously described.[1b]

*Dicarbonyl*($\eta^6$*-hexaethylbenzene*)(*trimethylphosphine*)*chromium*(0), (**5**). This complex was prepared by u.v. irradiation (1 h) of a freeze-thaw degassed heptane solution of (**2**) (0.44 g, 1.04 mmol) and $PMe_3$ (0.15 g, 2 mmol). The orange-yellow solution was filtered under $N_2$, the solvent evaporated and the residue extracted under $N_2$ with benzene. The solvent was removed under reduced pressure and the product recrystallised from benzene–heptane to give orange crystals (0.18 g, 41%). Complexes (**6**), (**7**), (**10**), and (**11**) were prepared in an exactly analogous way. Analytical figures are recorded in Table 1 for the previously unreported compounds.

*Dicarbonyl*($\eta^6$*-hexaethylbenzene*)(*thiocarbonyl*)*chromium*(0), (**4**). This complex was prepared by the method of McGlinchey *et al.*[2a]

*Dicarbonyl*($\eta^6$*-hexaethylbenzene*)(*triphenyl phosphite*)*chromium*(0), (**9**). This complex was supplied by Professor I. D. Rae.

($\eta^5$*-Cyclopentadienyl*)($\eta^6$*-hexaethylbenzene*)*iron*(II) *hexafluorophosphate*, (**12**). This complex was prepared by the method of Astruc and co-workers.[2b]

*Variable-temperature N.M.R. Measurements.*—All variable-temperature n.m.r. spectra were recorded at 90.1 MHz ($^{13}C$) or 145.87 MHz ($^{31}P$) on a Bruker WH360 spectrometer operating in the Fourier transform mode. All n.m.r. samples were filtered under $N_2$ through a grade 3 glass sinter, freeze-thaw degassed, and sealed in 10-mm (outside diameter) tubes. The temperature of the probe was measured by a thermocouple inserted in an n.m.r. tube filled with toluene to the same depth as the solution in the sample tube. Temperatures were considered accurate to ±2 °C.

Concentrations of the sample solutions were in the range 65—125 mmol $dm^{-3}$ and, except for (**12**), all samples were dissolved in $CD_2Cl_2$. Provided that they were carefully filtered, degassed, and the tube sealed, it was usually possible to supercool the solutions to at least 20 °C below the nominal freezing point of the solvent $CD_2Cl_2$, the samples remaining liquid for several hours at these temperatures.

Spectral simulations were performed using a version of the DNMR3 program[13] modified to handle single spin, n-site exchange. Satisfactory fit of simulated to observed spectra was judged by visual comparison. $\Delta G^‡$ Values were calculated using the Eyring equation.

*Crystallography.*—Crystals of (**11**), $C_{24}H_{32}MoO_5$, $M = 496.5$, obtained by slow evaporation of a heptane solution, are orthorhombic, space group $P2_12_12_1$, $a = 16.380(8)$, $b = 15.130(9)$, $c = 8.991(4)$ Å, $U = 2\,228.2$ Å$^3$, $D_m$ (flotation, $CHBr_3$–EtOH) = 1.47, $Z = 4$, $D_c = 1.48$ g $cm^{-3}$, Cu-$K_\alpha$ radiation, $\lambda = 1.5418$ Å, $\mu$(Cu-$K_\alpha$) = 51.1 $cm^{-1}$, $F(000) = 1\,016$. Multi-film equi-inclination Weissenberg photographs of reciprocal lattice layers 0—2 *k l*, *h* 0—2 *l*, and *h k* 0—6 were scanned by use of a microdensitometer (S.E.R.C. Daresbury Laboratory); 1 545 unique reflections were above background.

Absorption corrections were performed with the SHELX sub-program ABSC,[14] which uses the dimensions of the crystal between specified bounding faces together with the composition per unit cell and atomic absorption coefficients. For the three crystals used in this work, bounding faces and interface differences (mm) were: (i) ±[100], 0.25; ±[010], 0.15; ±[001], 0.15; (ii) ±[100], 0.24; ±[010], 0.39; ±[001], 0.31; and (iii) ±[110], 0.20; ±[−110], 0.20; ±[001], 0.37. Minimum and maximum transmission factors were 0.257, 0.536; merging $R = 0.054$.

The assignment of an absolute configuration from film data collected with Cu radiation from three crystals of uncertain relative handedness appeared to be unjustified. Therefore Friedel pairs were merged during data collection.

The approximate positions of the Mo atom were obtained from a Patterson synthesis and the carbon and oxygen atoms were located from a series of difference syntheses. Some trouble was experienced with false symmetry, due apparently to the alignment of the molecular pseudo-triad axis near the plane $y = \frac{1}{4}$. Full-matrix least-squares refinement converged at $R = 0.065$, $R' = 0.095$ $\{R' = [\Sigma w(\Delta F)^2/\Sigma wF^2]^{\frac{1}{2}}$; 126 parameters, Mo anisotropic, C and O isotropic, weighting factor in last cycle given by $w = 4.92(1 + 0.001\,18F^2)^{\frac{1}{2}}\}$. When C and O atoms were given anisotropic thermal parameters a number of thermal ellipsoids of C atoms became non-positive-definite. No hydrogen atoms could be located, but the final difference synthesis confirmed the absence of lattice solvent molecules and of any disorder in the ethyl groups. The SHELX 76 program[14] system was used in all calculations.

Selected bond lengths and angles are given in Table 4; deviations from the mean planes of the cyclic moieties are in Table 5; final atomic co-ordinates are in Table 6.

## Acknowledgements

We thank Dr. D. Reed of the S.E.R.C. High Field NMR Facility at the University of Edinburgh for obtaining the 90.1-MHz $^{13}C$

and 145.79-MHz $^{31}P$ n.m.r. spectra, Miss Stella Denholm for experimental assistance, and the Carnegie Trust for a Travel Grant (to G. H.). The work at Princeton was supported by the National Science Foundation.

## References

1 (*a*) G. Hunter, D. J. Iverson, K. Mislow, and J. F. Blount, *J. Am. Chem. Soc.*, 1980, **102**, 5942; (*b*) D. J. Iverson, G. Hunter, J. F. Blount, J. R. Damewood, jun., and K. Mislow, *ibid.*, 1981, **103**, 6073; (*c*) G. Hunter, J. F. Blount, J. R. Damewood, jun., D. J. Iverson, and K. Mislow, *Organometallics*, 1982, **1**, 448; (*d*) J. F. Blount, G. Hunter, and K. Mislow, *J. Chem. Soc., Chem. Commun.*, 1984, 170; (*e*) G. Hunter and K. Mislow, *ibid.*, p. 172.

2 (*a*) M. J. McGlinchey, J. L. Fletcher, B. G. Sayer, P. Bougeard, R. Faggiani, C. J. L. Lock, A. D. Bain, C. Rodger, E. P. Kundig, D. Astruc, J-R. Hamon, P. L. Maux, S. Top, and G. Jaouen, *J. Chem. Soc., Chem. Commun.*, 1983, 634; (*b*) J-R. Hamon, D. Catheline, D. Astruc, and M. J. McGlinchey, *J. Am. Chem. Soc.*, 1982, **104**, 7549; (*c*) M. J. McGlinchey, P. Bougeard, B. G. Sayer, R. Hofer, and C. J. L. Lock, *J. Chem. Soc., Chem. Commun.*, 1984, 789.

3 M. Crocker, M. Green, A. G. Orpen, and D. M. Thomas, *J. Chem. Soc., Chem. Commun.*, 1984, 1141.

4 R. K. Pomeroy and D. J. Harrison, *J. Chem. Soc., Chem. Commun.*, 1980, 661.

5 M. Acampora, A. Ceccon, M. Dal Farra, G. Giacometti, and G. Rigatti, *J. Chem. Soc., Perkin Trans. 2*, 1977, 483.

6 C. A. Tolman, *J. Am. Chem. Soc.*, 1970, **92**, 2956.

7 R. F. Childs, A. Varadarajan, C. J. L. Lock, R. Faggiani, C. A. Fyfe, and R. E. Wasylishen, *J. Am. Chem. Soc.*, 1982, **104**, 2452.

8 E. M. Campi, B. M. K. Gatehouse, W. R. Jackson, I. D. Rae, and M. G. Wong, *Can. J. Chem.*, 1984, **62**, 2566.

9 T. A. Albright, P. Hoffmann, and R. J. Hoffmann, *J. Am. Chem. Soc.*, 1977, **99**, 7546 and refs. therein; P. Delise, G. Allegra, E. R. Mognaschi, and A. Chierico, *J. Chem. Soc., Faraday Trans. 2*, 1975, 207; W. R. Jackson, C. F. Pincombe, I. D. Rae, D. Rush, and B. Wilkinson, *Aust. J. Chem.*, 1976, **24**, 2413.

10 H. A. Patel, A. J. Carty, M. Mathew, and G. J. Palenik, *J. Chem. Soc., Chem. Commun.*, 1972, 810.

11 Yu T. Struchkov, V. G. Andrianov, V. N. Setkina, N. K. Baranetskaya, V. J. Losilkina, and D. N. Kursanov, *J. Organomet. Chem.*, 1979, **182**, 213.

12 K. A. Woode, J. C. J. Bart, M. Calcaterra, and G. Agnes, *Organometallics*, 1983, **2**, 627.

13 G. Binsch and D. A. Kleier, Quantum Chemistry Program Exchange, Indiana University, 1970, vol. 11, no. 165.

14 G. M. Sheldrick, SHELX 76 Program for Crystal Structure Determination, University of Cambridge, 1975.

*Received* 18*th March* 1985; *Paper* 5/455